Nanoindentation: Depth dependence of silicon hardness studied within contact theory

M. Hebbache
Laboratoire de Physique Théorique de la Matière Condensée, Université Paris 7 - Denis Diderot, 2 Place Jussieu, F-75251 Paris Cedex 05, France

(Received 11 April 2003; published 12 September 2003)

The behavior of elastic and mechanical properties of silicon submitted to an indentation test is investigated. The study is focused on the behavior of its hardness at the nanoscale. For this aim, we apply a Green-function approach for solving the contact problem of elastic bodies. The anisotropy of the two contacting materials, silicon and a diamond indenter, is taken into account for obtaining the depth dependence of the hardness up to about 90 nm at which the semiconductor-metal phase transition occurs. It is shown that the discrepancy with experimental data can be significantly reduced if one takes into account the anharmonicity of the materials in contact. The anisotropy is represented by the full tensor of second-order elastic constants C_{IJ} and the anharmonicity by the full tensors of higher-order elastic constants $C_{IJK\ldots}$. The validity of the theoretical approach was checked by determining the force-depth indentation curve.

DOI: 10.1103/PhysRevB.68.125310 PACS number(s): 62.20.Dc, 05.30.Fk, 71.15.Nc

I. INTRODUCTION

Nanoscale experimental techniques reveal unusual physical properties which are not fully understood. The indentation is a technique which allows the measurement of hardness by pressing an indenter into a flat surface of the material and measuring the size of the impression. It has been extended to the micrometer and nanometer scale through the use of depth-sensing indentation equipment.[1] This instrument records the applied load and the displacement of the indenter throughout the indentation process. The analysis of the load-penetration curve allows the determination of a number of useful engineering properties. Nanoindentation has become a well-established technique for the investigation of mechanical properties of materials and the Olivier-Pharr approach,[2] which expands the ideas developed by Loubet *et al.*[3] and Doerner and Nix,[4] the standard technique of data analysis. Understanding the mechanical properties of materials at the nanoscale is crucial for applications. The intrinsic mechanical behavior of semiconductors is of particular interest because they are widely used for the fabrication of electronic devices which operate in large ranges of stresses and temperatures. The performances of these devices can be significantly degraded due to contact loading during processing or use. Hard semiconductors are intensively investigated because of their potential use in extreme conditions.[5] Silicon, which is a relatively hard material, has already found new applications in micro- and nano-electro-mechanical systems (MEMS and NEMS). In previous papers, we have studied the sequence of phase transitions, diamond $\Rightarrow \beta$-Sn$\Rightarrow$ *Imma* structure, which occurs in silicon during high-pressure experiments[6] and indentation tests.[7] The first structural transformation makes in evidence two electrically and geometrically different states. The parent phase has a diamond structure (Si I) and is semiconductor while the new phase is tetragonal and metallic (Si II). On pressure release, the diamond structure is not reconstructed. A rhombohedral structure takes place ($R8$) on slow decreasing pressure. The reversible phase transition[8] exists between the $R8$ phase and the bcc phase ($BC8$ or Si III). The nonreversibility of the Si I$\Rightarrow$Si II phase transition hinders the appearance of new applications like detectors of ultralow forces or impacts. The present work is focused on the elastic and mechanical behavior of a thin film of silicon. The main aim is to predict the evolution of its hardness when it is indented to nanometer-scale depth. From the theoretical point of view, indentation is a contact problem which has been only partially solved. To date, there is no complete quantitative theory of hardness of semiconductors. Much of the theoretical works are restricted to isotropic solids. Little attention has been paid to anisotropy, anharmonicity, and structural transformations which occur beneath the indenter. In materials science and engineering, the elastic modulus are systematically assumed to be stress independent. Their discontinuity at the phase transition points is also ignored. The same number of elastic modulus are considered on both sides of the phase transition. For instance, the cubic phase of silicon (Si I) has three independent elastic constants while its tetragonal phase (Si II) possesses six. The presence and the nonreversibility of phase transitions are not taken into account in the data analysis. Some of the above-mentioned issues have been considered in Refs. 6 and 7. Others issues are under consideration in the present study. The paper is organized as follows. The main formulas for describing the indentation are reviewed in the second section. The numerical results are given in the third section.

II. THEORY

It is commonly accepted that the hardness characterizes the material resistance to elastic and plastic deformation. Nanoindentation tests show that the responses of silicon[9] and diamond[10] are largely elastic under low applied loads. These covalent crystals can, in principle, deform plastically, although usually at higher temperatures and higher stresses than metals.[11] In what follows, we will study the elastic response of silicon when it is pressed by a diamond spherical indenter. Comparison with experimental data will give an order of magnitude of the plastic response in silicon. The indentation problem, which is associated with the names of Hertz[12] and Boussinesq,[13] is one of contact problems of elas-

TABLE I. Measured second- and third-order elastic constants of silicon and diamond, in unit of Mbar, and elastic compliances S_{IJ} in unit of Mbar^{-1}. The theoretical values of the fourth-order elastic constants obtained by three groups are different.

Material	C_{11}	C_{12}	C_{44}	C_{111}	C_{112}	C_{123}	C_{144}	C_{166}	C_{456}	Ref.	
Silicon	16.57	6.39	7.96	−82.5	−45.1	−6.4	1.2	−31	−6.4	21	
	16.56	6.39	7.95	−79.5	−44.5	−7.5	1.5	−31	−8.6	22	
Diamond	107.6	12.5	57.7	−626.0	−226.0	11.2	−67.40	−286.0	−82.3	23	
	107.9	12.4	57.8							21	
	S_{11}	S_{12}	S_{44}								
Silicon	0.7680	−0.2138	1.2559							34	
Diamond	0.0949	−0.0098	0.1742							21	
	C_{1111}	C_{1112}	C_{1122}	C_{1123}	C_{1144}	C_{1155}	C_{1244}	C_{1266}	C_{1456}	C_{4444}	C_{4455}
Silicon	51	158	−156	53	−149	−229	186	−92	5.8	−347	14 [a]
	≈0	32 [b]									
	122 [c]										
Diamond	436	302							53 [d]		

[a]Reference 29.
[b]Reference 31.
[c]Reference 32.
[d]Reference 35.

tic bodies. An elegant solution of this problem has been given by Sneddon.[14] The author used the Hankel transform and the theory of dual integral equations for solving the equilibrium equations of a strained material. Unfortunately, Sneddon's solution is only valid for isotropic materials. The anisotropy of a cubic material is usually represented by the ratio of its shear modulus, i.e., $\zeta=(C_{11}-C_{12})/2C_{44}$. C_{IJ} is the contracted notation of Voigt for the fourth-order tensor of second-order elastic constants C_{ijkl}. ζ is equal to 0.64 for silicon, 0.82 for diamond, and 1.0 for an isotropic material (see Table I). In what follows, we apply the Hertzian contact theory of anisotropic materials.[15] In place of the two Lame coefficients or their equivalents, the full tensor C_{ijkl} is considered. We consider a Cartesian coordinate system which coincides with the cubic system. The origin of the coordinates and the x_1 and x_2 axes are on the free surface; and the x_3 axis is along the fourfold symmetry axis [001]. The half space $x_3>0$, occupied by silicon, is loaded by a diamond spherical indenter. The stress-induced displacement field **u** in silicon can be written in the form[16]

$$u_k(\mathbf{r})=\int_A G_{ks}(\mathbf{r}-\mathbf{r}')p_s(\mathbf{r}')d\mathbf{r}', \tag{1}$$

where $p_s(\mathbf{r})$ is the pressure distribution beneath the indenter and $G_{ks}(\mathbf{r})$ the elastostatic Green function for a semi-infinite anisotropic material, i.e., the displacement at point **r** in the direction k due to a unit force at point $\mathbf{r}'$ in the direction s. The integration is over the projected contact area A. Due to the fourfold symmetry axis perpendicular to the free surface of silicon, A is a circular area. In linear elasticity, $G_{ks}(\mathbf{r})$ is solution of the equilibrium equation,[15,17]

$$C_{ijkl}\frac{\partial^2 G_{ks}(\mathbf{r})}{\partial x_l \partial x_j}=0. \tag{2}$$

The usual convention regarding summation on repeated subscripts is used. First, we consider that C_{ijkl} are stress independent, as commonly used. In the two-dimensional (2D) Fourier space, a possible solution of Eq. (2) is[15,17]

$$\tilde{G}_{ks}(\mathbf{K},x_3)=\sum_\alpha \varepsilon_{k\alpha}(\mathbf{K})\chi_{\alpha s}(\mathbf{K})e^{-im_\alpha K x_3} \tag{3}$$

with $i^2=-1$. K is the magnitude of the 2D vector **K**. m_α are complex conjugate pairs roots of the sixth-order determinantal equation of Stroh,[18]

$$|\Gamma_{ik}^\alpha|=|C_{ijkl}(q_l+n_l m_\alpha)(q_j+n_j m_\alpha)|=0, \tag{4}$$

with $\mathbf{q}=\mathbf{K}/K$. **n** is the inward normal to the free surface. In Eq. (3), $\varepsilon_{k\alpha}$ are the components of the corresponding normalized eigenvectors,

$$\Gamma_{ik}^\alpha \varepsilon_{k\alpha}=0. \tag{5}$$

There is no sum over α. The coefficients $\chi_{\alpha s}$ are determined form the boundary condition at the free surface $x_3=0$:

$$n_j C_{ijkl}(\partial G_{ks}/\partial x_l)=-\delta_{is}\delta(x_1)\delta(x_2). \tag{6}$$

δ_{is} is the Kronecker's symbol and $\delta(x_j)$ the Dirac's function. Only the roots m_α in the lower half of the complex plane must be considered in Eq. (3) in order to fulfill the decay

condition, i.e., $u_k \to 0$ as $x_3 \to \infty$. The propagation of surface waves in anisotropic elastic materials can be studied in a similar way.[19] One should consider the wave equation, i.e., include the time-dependent term $\rho[\partial^2 G_{is}(\mathbf{r})/\partial t^2]$, on the right-hand side of Eq. (2). ρ is the mass density. In the language of lattice dynamics, $\mathbf{K}$ is the in-plane wave vector, $\varepsilon_{k\alpha}$ the polarization vector, and $\chi_{\alpha s}$ the weighting factor. In real space, the elastostatic Green function is given by

$$G_{ks}(\mathbf{r}) = \frac{K^3}{4\pi^2}\int_0^{2\pi}\sum_{\alpha}\ \varepsilon_{k\alpha}(\phi)\chi_{\alpha s}(\phi) \times[\mathbf{q}\cdot\mathbf{x} + m_\alpha(\phi)x_3]^{-1}d\phi \tag{7}$$

with $\mathbf{r}=(\mathbf{x},\ x_3)$. $\mathbf{r}$ gives the position of a material point. $\mathbf{x}$ is the 2D vector with components x_1 and x_2. ϕ is the angle between the directions of $\mathbf{q}$ and $\mathbf{x}$. It has been proved that the Hertz's pressure distribution is also valid for anisotropic materials,[15,16] i.e., $p_s(\mathbf{x}) = p_o(1 - x^2/\xi^2)^{1/2}$ with $x = |\mathbf{x}|$ and $p_o = 3F/2\pi\xi^2$. F is the applied force and ξ the radius of the projected contact area. Substituting such expression of p_s and that of the surface Green function $G_{ks}(\mathbf{x}, x_3 = 0)$ into Eq. (1) and performing the integration over A, one obtains the displacement of the free surface of silicon $u_3^{Si}(\mathbf{x}, x_3 = 0)$.[15] The procedure must be repeated for obtaining the displacement of the surface of the spherical indenter in contact with silicon. The contact area is in general elliptical unless the surface possesses a fourfold symmetry axis, at least. An average over various planes of diamond would give more accurate results. However, for the sake of simplicity, we have considered that it is the (001) plane of diamond which is in contact with silicon. The relative displacement of the two materials, at the origin, is given by[15] (see also Ref. 16)

$$\delta = \sum_{\lambda=1}^{2} u_3^{\lambda}(\mathbf{x}) + x^2/2\mathcal{R} \tag{8}$$

$$= (F/\xi)\sum_{\lambda=1}^{2} I_\lambda \tag{9}$$

$$= \xi^2/\mathcal{R} \tag{10}$$

with

$$I_\lambda = \frac{3}{16\pi}\int_0^{2\pi}\sum_{\alpha=1}^{3} K\chi_{\alpha 3}(\phi)\varepsilon_{3\alpha}(\phi)d\phi. \tag{11}$$

In Eqs. (8) and (9), the summation is over the contacting materials and $\mathcal{R}$ is the radius of the spherical indenter.

III. NUMERICAL RESULTS

For comparison with the experimental results of Williams *et al.*,[20] we have considered a diamond spherical indenter with a radius $\mathcal{R}$ equal to 4.2 μm. The constants $C_{ijkl} = C_{IJ} = \rho v^2$ involved in the above equations have been deduced from the measurement of the ultrasonic velocities v of the bulk elastic waves[21–23] (see Table I). The construction of the 3×3 matrix Γ_{ik}^{α} [Eq. (4)] for silicon and diamond is laborious but straightforward. The vanishing of the determinant of Γ_{ik}^{α} leads to a cubic equation in m_α^2. The three acceptable complex roots m_α for the (001) plane of Si I can be readily obtained. Their variations are shown in Fig. 1. The corresponding normalized eigenvectors $\varepsilon_{k\alpha}$ and the weighting factors $\chi_{\alpha s}$ have been computed using the package Mathematica.[24] Figure 2 shows the variations of $M_{\alpha 3} = K\chi_{\alpha 3}$ in silicon. Similar results have been found for diamond. The contour integral (11) can be then calculated. It is equal to 4521.5 for silicon and 667.5 $\mathrm{mN^{-1}\,nm^2}$ for diamond. Figure 3 gives the force vs penetration depth curve [see Eq. (9)]. The agreement with the experimental data of Williams *et al.*[20] is satisfactory. This confers a certain valid-

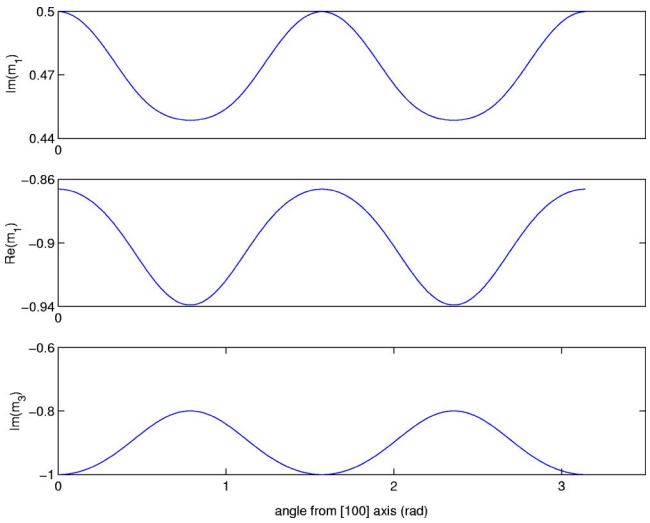

FIG. 1. Variations in the (x_1, x_2) plane of the contributing roots $m_\alpha(\phi)$ to the elastic Green function of silicon using the zero-stress elastic constants C_{IJ}. m_3 is purely imaginary, $\mathrm{Re}(m_2) = -\mathrm{Re}(m_1)$ and $\mathrm{Im}(m_2) = \mathrm{Im}(m_1)$. The angle ϕ is measured from x_1 axis coinciding with the [100] fourfold symmetry axis. Similar results have been found for diamond.

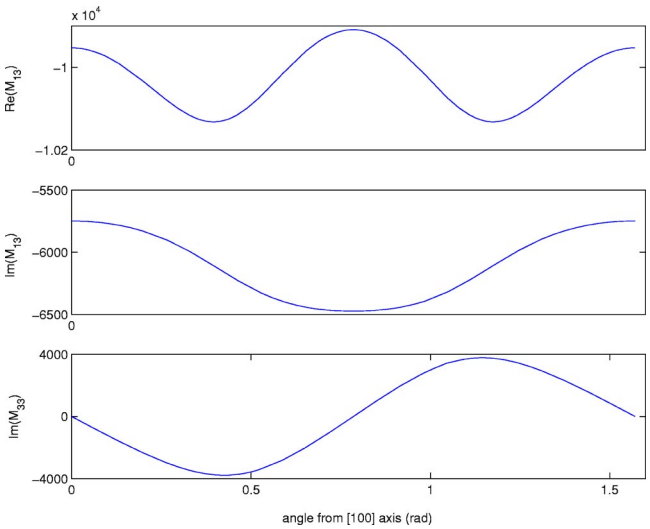

FIG. 2. Variations of the weighting factors $M_{\alpha 3} = K\chi_{\alpha 3}(\phi)$. M_{33} is purely imaginary, $\mathrm{Re}(M_{23}) = -\mathrm{Re}(M_{13})$ and $\mathrm{Im}(M_{23}) = \mathrm{Im}(M_{13})$.

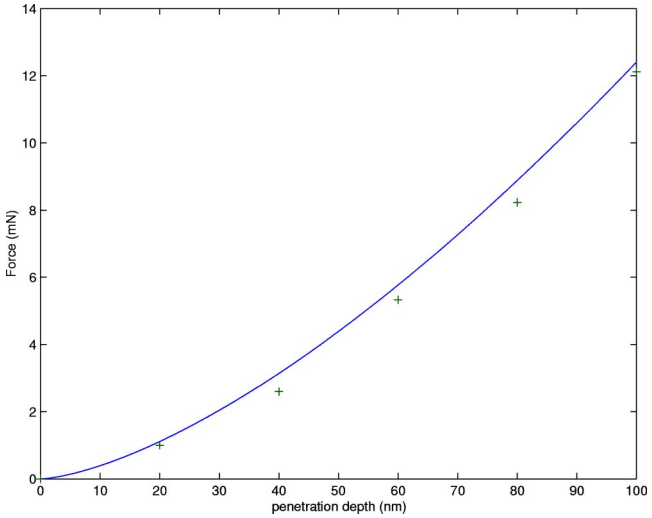

FIG. 3. Force versus penetration depth. Crosses are experimental data (Ref. 20) obtained with a 4.2-μm diamond spherical indenter on (001) Si I.

ity to the approach. The hardness is defined as $H=F/A$. It can be rewritten in the form

$$H=\frac{\sqrt{\delta/\mathcal{R}}}{\pi I} \tag{12}$$

with $I=\Sigma_{\lambda=1}^{2} I_{\lambda}$. The sommation is over the contacting materials. The broken line in Fig. 4 is the hardness vs depth curve. The experimental results of Williams *et al.*[20] are reported on the same figure (crosses). The broken line is obtained with stress independent C_{IJ}. The discrepancy between experimental and calculated values of H increases on loading. It reaches its maximum at the penetration depth of about 90–100 nm at which the metallization of silicon occurs. Such discrepancy can be reduced significantly if one takes into account the harmonicity of materials. This can be achieved through the stress dependence of the harmonic elastic constants C_{IJ}. The effect of uniaxial stress on bulk ultrasonic waves have been studied by Thurston and Brugger[25] (see also Ref. 26). The authors established a general expression for the stress dependence of elastic constants of arbitrary crystal symmetry:

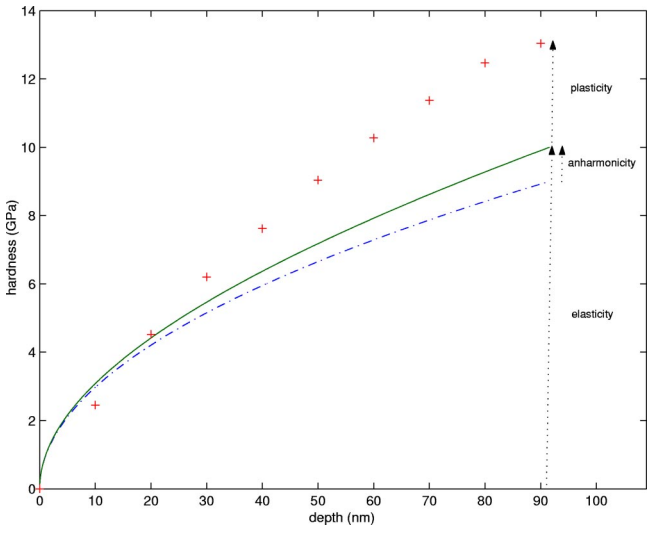

FIG. 4. Hardness of the (001) plane of Si I vs penetration depth. Crosses are experimental data (Ref. 20). The broken line and the continuous line represent Eq. (6) with the contour integral I equal to 5189 and $(5189-32.27p_o)$, respectively. I is in unit of $\mathrm{mN}^{-1}\,\mathrm{nm}^2$ and p_o in GPa.

$$C_{IJ}(\sigma)=C_{IJ}(0)+\lambda_{IJ}\sigma+\Pi_{IJ}\sigma^2+\cdots. \tag{13}$$

σ is the magnitude of the applied stress, assumed to be uniform by the authors,[25,26] i.e., $\sigma=p_o$. At low load, the anharmonicity is mainly represented by the second term on the left-hand side of Eq. (13). The coefficient λ_{IJ} involves third-order elastic constants, $C_{ijklmn}=C_{IJK}$. The third term on the left-hand side of Eq. (13), involves fourth-order elastic constants $C_{ijklmnpq}=C_{IJKL}$. In the case of silicon, its magnitude should become significant on approaching the diamond$\Rightarrow\beta$-Sn phase transition because it is indispensable for describing the stability of the metallic β-Sn phase, as shown in Ref. 7. The reason is the following. According to Musgrave and Pople,[27] the Si I$\Rightarrow$Si II structural transformation is due the tetragonal shear strain $\eta\sim(2e_{33}-e_{11}-e_{22})$. $e_{ii}=\partial u_i/\partial x_i$ are the diagonal components of the strain tensor and express the relative variations of the lattice parameters. η is a shear strain which reduces the dimension of one of the cubic axes and expands the other two, leading to the tetragonal structure of β-Sn (Si II). An expansion of the deformation energy up to fourth order, at least, is required for studying such displacive phase transition of first order: $U(\eta)-U(0)=\Sigma_{n=2}^{N\geq 4}C_n\eta^n$. C_n are effective elastic constants associated with the tetragonal strain. They are combinations of the nth-order elastic constants and are related to the nth-order bond-bending force constants which tend to stabilize the equilibrium angle between covalent bonds.[28,29] The analytic expressions of the coefficients λ_{IJ} and Π_{IJ} appearing in Eq. (13) can be found in Refs. 25 and 26. Their calculation requires also elastic compliances S_{IJ} (see Table I). Third-order elastic constants C_{IJK} are obtained from the measurements of ultrasonic velocity changes due to uniaxial stresses. Their values are listed in Table I. McSkimin and Andreatch[21] have found that these velocities vary linearly with applied stresses. Deviations from the linear change have been detected by Suzuki *et al.*[30] This supports the fact that the quadratic term, $\Pi_{IJ}\sigma^2$, which appears in Eq. (13) is not negligible. Its computation requires the knowledge of the fourth-order elastic constants C_{IJKL}. The latter can be measured by means of shock wave techniques. In the literature, we just find the calculated values of C_{IJKL} (see Table I). In the case of silicon, the values obtained by Nielsen and Martin[31] using *ab initio* calculations differ largely from that obtained by Gerlich[29] who applied a generalized Keating model. A third approach has been used by Prasad and Suryanarayana[32] to calculate C_{1111} of silicon. For lack of reliable values of C_{IJKL}, we limit the expansion (13) to first order. The anharmonicity of the materials will be then only represented by the third-order elastic constants in this work. The variations of C_{IJ} in the cubic phase of silicon (Si I) are

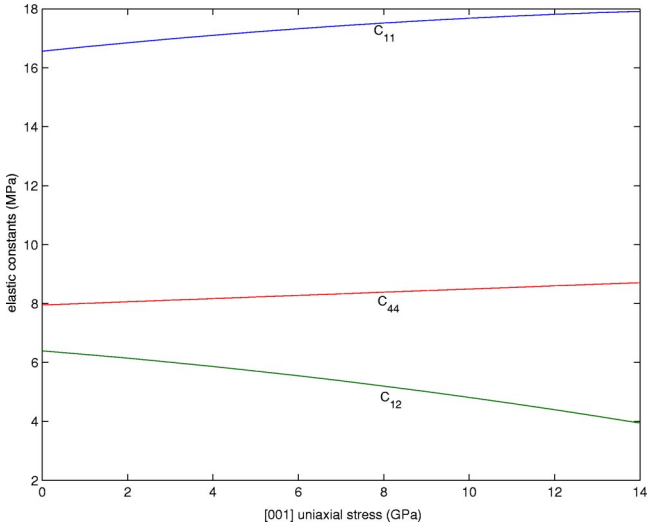

FIG. 5. Variations of harmonic elastic constants of Si I under a uniaxial stress.

shown in Fig. 5. Diamond is the hardest material and its second-order elastic constants are almost stress independent. We find that the contour integrals I_λ involved in Eq. (9) vary approximately as follows: $I_1 = I_{Si} \approx 4521.5 - 32.54 p_o$ and $I_2 = I_C \approx 667.5 + 0.27 p_o$. p_o is in unit of GPa. For diamond, the integral (11) is almost constant in the pressure range 0–14 GPa, i.e., the stability range of the cubic phase of silicon.[33]

IV. CONCLUSION

We applied the Hertzian contact theory for studying the hardness of a thin film of silicon. We have taken into account the anisotropy of the two contacting materials, i.e., silicon and diamond. All the parameters (roots of the determinantal equation of Stroh, polarization vectors, weighting factors) which allow us to calculate the elastic Green function of the (001) plane of silicon have been given. The procedure has been repeated to include the characteristics of the indenter. Using the Hertz's pressure distribution, we computed the integral (1) for obtaining the displacements of the free surfaces in contact. The anharmonicity of the materials has been taken into account approximately by using a renormalization of second-order elastic constants [Eq. (13)]. Only the measured third-order elastic constants have been considered in such renormalization. The omission of higher-order anharmonic terms reduces slightly the accuracy of the numerical results. However, they are essential for stabilizing the metallic phase. An acceptable agreement has been found between the calculated and the experimental force-penetration depth curves. The discrepancy between the calculated and the measured hardness of silicon has been reduced by including the anharmonicity of silicon. The agreement between the measured and the calculated hardness could be improved by including the plastic deformation. Unfortunately, plastic deformation produces in silicon a complex structure of lattice defects which is presented in many excellent reviews (see, for example, Ref. 36). We already showed that impurities affect weakly the elastic constant C_{44} of group-IV semiconductors.[37] Attempts to involve dislocations in the behavior of physical properties of materials, in presence or absence of phase transitions, were made by various authors.[38] It is expected that dislocations induce ultrasonic attenuation and velocity change,[39] or equivalently, a renormalization of C_{IJ}, specially in silicon which undergoes a phase transition driven by a soft elastic wave. Unfortunately, these theories based on simplifying assumptions cannot be applied to silicon which exhibits various forms of dislocations. In this semiconductor, the dislocations can be straight, heavily kinked or jogged, clean or decorated with impurities, and are generally dissociated into partials separated by a stacking fault. However, the understanding of plasticity in semiconductors is in constant progress.

[1] J.N. Pethica, R. Hutchings, and W.C. Olivier, Philos. Mag. A **48**, 598 (1983).
[2] W.C. Olivier and G.M. Pharr, J. Mater. Res. **7**, 1564 (1992).
[3] J.L. Loubet, J.M. Georges, O. Marchesini, and G. Meille, J. Tribol. **106**, 43 (1984).
[4] M.F. Doerner and W.D. Nix, J. Mater. Res. **1**, 601 (1986).
[5] J. Isberg, J. Hammaersberg, E. Johansson, T. Wikstrom, D.J. Twitchen, A.J. Whitehead, S.E. Coe, and G.A. Scarsbrook, Science **297**, 1657 (2002).
[6] M. Hebbache, M. Mattesini, and J. Szeftel, Phys. Rev. B **63**, 205201 (2001).
[7] M. Hebbache and M. Zemzemi, Phys. Rev. B **67**, 233302 (2003).
[8] J. Crain, G.J. Ackland, J.R. Maclean, R.O. Piltz, P.D. Hatton, and G.S. Pawley, Phys. Rev. B **50**, 13 043 (1994).
[9] J. Woirgard, C. Thomas, J.C. Girard, and V. Audurier, J. Eur. Ceram. Soc. **18**, 2297 (1998).
[10] A. Richter, R. Ries, R. Smith, M. Henkel, and B. Wolf, Diamond Relat. Mater. **9**, 170 (2000).
[11] J. Castaing, P. Veyssiere, L.P. Kubin, and J. Rabier, Philos. Mag. A **44**, 1407 (1981).
[12] H. Hertz, J. Reine Angew. Math. **92**, 156 (1882).
[13] J. Boussinesq, *Application Des Potentiels à l'Étude de l'Équilibre et du Mouvement des Solides Élastiques* (Gauthiers-Villars, Paris, 1885).
[14] I.N. Sneddon, in *Fourier Transforms* (McGraw-Hill, New York, 1951); I.N. Sneddon, Int. J. Eng. Sci. **3**, 47 (1965).
[15] J.R. Willis, J. Mech. Phys. Solids **14**, 163 (1966).
[16] L. Landau and E. Lifchitz, *Theory of Elasticity* (Pergamon Press, London, 1970).
[17] D.M. Barnett and J. Lothe, Phys. Norv. **8**, 13 (1975).
[18] A.N. Stroh, Philos. Mag. **3**, 625 (1958); J. Math. Phys. **41**, 77 (1962).
[19] G.W. Farnell, in *Physical Acoustics* (Academic Press, New York, 1970), Vol. 6, p. 109.
[20] J.S. Williams, Y. Chen, J. Wong-Leung, A. Kerr, and M.V. Swain, J. Mater. Res. **14**, 2338 (1999).

[21] H.J. McSkimin and P. Andreatch, Jr., J. Appl. Phys. **35**, 3312 (1964); **43**, 2944 (1972).
[22] J.J. Hall, Phys. Rev. **161**, 756 (1967).
[23] M.H. Grimsditch, E. Anastassakis, and M. Cardona, Phys. Rev. B **18**, 901 (1978); M.H. Grimsditch and A.K. Ramdas, *ibid.* **11**, 3139 (1975).
[24] S. Wolfram, *Mathematica: A System for Doing Mathematics by Computer* (Addison-Wesley, Palo Alto, 1991).
[25] R.N. Thurston and K. Brugger, Phys. Rev. **133**, A1604 (1964).
[26] D.C. Wallace, in *Solid State Physics*, edited by F. Seitz and D. Turnbull (Academic, New York, 1970), Vol. 25, p. 301.
[27] M.J.P. Musgrave and J.A. Pople, J. Phys. Chem. Solids **23**, 321 (1962).
[28] D. Vanderbilt, S.H. Taole, and S. Narasimhan, Phys. Rev. B **40**, 5657 (1989).
[29] D. Gerlich, J. Appl. Phys. **77**, 4373 (1995).
[30] T. Suzuki, B.B. Chick, and C. Elbaum, Appl. Phys. Lett. **7**, 2 (1965).
[31] O.H. Nielsen and R.M. Martin, Phys. Rev. B **32**, 3792 (1985).
[32] O.H. Prasad and M. Suryanarayana, Phys. Status Solidi B **112**, 627 (1982).
[33] S. Hainsworth, A.J. Whitehead, and T.F. Page, in *Plastic Deformation in Ceramics*, edited by R.C. Bradt, C.A. Brookes, and J. L. Routbart (Plenum Press, London, 1994), p. 173.
[34] C.S.G. Cousins, L. Gerward, J. Staun Olsen, B. Selsmark, and B.J. Sheldon, J. Phys. C **20**, 29 (1987).
[35] O.H. Nielsen, Phys. Rev. B **34**, 5808 (1986).
[36] H. Alexander, in *Dislocations in Solids*, edited by F.R.N. Nabarro (Elsevier, New York, 1986), Chap. 35, p. 115.
[37] M. Hebbache, Phys. Rev. B **49**, 6522 (1994).
[38] S.P. Obukhov, Sov. Phys. JETP **56**, 1144 (1982); Yu.M. Kishinets, A.P. Levanyuk, A.I. Morozov, and A.S. Sigov, Sov. Phys. Solid State **29**, 347 (1987); E.V. Balashova, V.V. Lemanov, and A.B. Sherman, Ferroelectrics **79**, 157 (1988).
[39] A. Granato and K. Lűcke, J. Appl. Phys. **27**, 583 (1956); **27**, 789 (1956); T. Suzuki and C. Elbaum, *ibid.* **35**, 1539 (1964); I.E. Dikshteĭn, V.V. Tarasenko, and V.D. Kharitonov, Sov. Phys. Solid State **21**, 1374 (1979); Yu.M. Kishinets, A.P. Levanyuk, A.I. Morozov, and A.S. Sigov, Ferroelectrics **79**, 27 (1988).